Clustering of instrumental methods to characterize the texture and the rheology of slimy okra (Abelmoschus esculentus) suspensions

Timoty Savouré, Manuel Dornier, Laurent Vachoud, Antoine Collignan

Savouré, T., Dornier, M., Vachoud, L., & Collignan, A. (2020). Clustering of instrumental methods to characterize the texture and the rheology of slimy okra (*Abelmoschus esculentus*) suspensions. *Journal of Texture Studies, 51*, 426-443. DOI: 10.1111/jtxs.12505

Short informative title: Clustering of instrumental methods to characterize the texture and the rheology of slimy okra (*Abelmoschus esculentus*) suspensions

Short running title: Rheology and texture of slimy okra sauces

Timoty SAVOURE [a,b], Manuel DORNIER [b], Laurent VACHOUD [b], Antoine COLLIGNAN [b,*]

[a] AS Food International, Grenoble, France

[b] Qualisud, Univ Montpellier, CIRAD, Montpellier SupAgro, Université d'Avignon, Université de La Réunion, Montpellier, France.

* Corresponding author.

Address: Cirad, UMR 95 Qualisud, 73, rue Jean François Breton, TA B-95/15, 34398 Montpellier cedex 5, France,

Tel.: + 33 4 67 61 6597

E-mail address: antoine.collignan@supagro.fr

BRIEF ABSTRACT FOR THE GRAPHICAL ABSTRACT

- Slimy okra suspensions are structured fluids with significant elongational properties.
- Measuring flow and stringy properties is sufficient to characterize their rheological and textural properties and necessary to discriminate them according to their processing and formulation.
- Rheological and textural properties are affected by formulation, drying and thermal processes.

ABSTRACT

Okra (*Abelmoschus esculentus)* is one of the ingredients widely used in African gastronomy because of the unique slimy texture it gives to sauces. However, processing and formulation can affect the textural and rheological properties of these sauces, leading to unacceptable quality for the African consumer. The aim of this study was to select the instrumental measurements best enabling i) characterization of the rheology and texture of slimy sauces prepared from okra and ii) monitoring its evolution during the preservation process. 37 slimy suspensions (sauces and purées) were measured with 16 rheological and textural parameters. A Principal Component Analysis revealed that flow consistency index K and flow behavior index n were well correlated with visco-elastic, adhesive and shear thinning properties, and that stringiness was well correlated with elongational, cohesive and ductile properties. These two sets of measurement methods are sufficient to characterize their rheological and textural properties, and necessary to discriminate them according to their process and formulation.

KEYWORDS

Okra, Slimy sauces, Stringiness, Structured fluid, Rheology, Texture

1. INTRODUCTION

Various plant-origin ingredients are traditionally used in West and Central African cuisine because of the slimy consistency they give to sauces, soups and stews. This is the case of okra (*Abelmoschus esculentus* (L.) Moench), nkui (bark of *Triumfetta pentandra* A. Rich) and dika nut kernels (*Irvingia gabonensis* (Aubry Lecomte ex O'Rorke)) (Kouebou *et al.*, 2013; Mateus-Reguengo *et al.*, 2019; Ndjouenkeu, Goycoolea, Morris, & Akingbala, 1996). For consumers in sub-Saharan Africa, one of the essential functions of slimy sauces is to facilitate the swallowing of the starchy dough they are served with (Owoeye, Caurie, Allagheny, & Onyezili, 1990). For them, the "slimy" properties of okra are its main attribute, and therefore an essential quality criterion (Uzo & Ojiako 1980).

Okra sauces have never undergone rheological and textural characterization, but many studies have focused on the rheological properties of okra extracts (mucilage, polysaccharides and pectins in particular). In addition to their sliminess, they have original thickening, shear thinning, viscoelastic and visco-elastic properties (Kontogiorgos, Margelou, Georgiadis, & Ritzoulis, 2012; Ndjouenkeu *et al.*, 1996; Sengkhamparn *et al.*, 2010), emulsifying properties (Kpodo *et al.*, 2018) and elongationnal properties (Yuan, Ritzoulis, & Chen, 2018) properties. The rheological properties of okra mucilage are the result of complex interactions between the various macromolecular populations of which it is composed (Ritzoulis, 2017), including very specific pectic compounds (Kpodo *et al.*, 2018).

The textural properties of okra products, including sauces, can be significantly altered by preparation and stabilization processes. Studies that investigated the impact of the process on the textural

properties of okra focused on the viscosity (simple, kinematic, relative) of its mucilage or okra sauces. They showed that the viscous properties of the product are degraded by drying (Falade & Omojola, 2010; Inyang & Ike, 1998), blanching (Inyang & Ike, 1998) and cooking (Woolfe, Chaplin, & Otchere, 1977). These effects on the rheological properties of okra are a major obstacle to the conservation of this vegetable before consumption in West Africa. In order to improve the processing conditions of this vegetable, it is therefore essential to have tools that allow the best enabling assessment of its slimy properties.

Only a few old studies took an interest in the instrumental measurement of the slimy texture of food. For Uzo & Ojiako (1980), the perception of the sliminess of a whole okra is correlated with the kinematic viscosity of its mucilage. Other authors have shown correlations between the perception of sliminess in the mouth and the shear thinning (Szczesniak & Farkas, 1962; Wood, 1974) or viscous properties (Richardson *et al.*, 1989) of a food, while some did not find a correlation (Terpstra *et al.*, 2009). As a result, no clear and consistent trend emerges from these sometimes contradictory results. Moreover, measurements of viscous properties alone do not seem sufficient to appraise the quality of slimy sauces, since African consumers base their assessment on their ability to elongate it (Fasogbon, Taiwo, & Adeniran, 2017; Leakey *et al.*, 2005). Finally, for Szczesniak & Farkas (1962), "*a slimy material was defined as one that is thick, coats the mouth, and is difficult to swallow*". But this definition seems to contradict the fact that for African consumers, slimy sauces facilitate swallowing.

In this context, the objective of this study is to select the instrumental measurements best enabling i) characterization of the texture of slimy sauces prepared from okra and ii) monitoring its evolution during the preservation process. The proposed strategy was to measure the rheological and textural properties of a wide range of samples of okra purées and sauces using different experimental methods described in the literature. These methods were then compared with each other to extract the most relevant instrumental parameters.

2. MATERIALS AND METHODS

2.1. Sample generation

In order to obtain slimy suspensions with the greatest possible variety of rheological and textural properties, 37 samples were prepared by varying the formulation and using processes known to have an impact on the texture of okra (Figure 1).

Two batches of fresh okra purée were prepared and frozen. Of these, 36 samples were formulated at different pH and dry matter contents (no.1-31), mixed with other slimy ingredients (no.32-33) or used in a traditional recipe (no.34-36). These preparations could then be cooked (no.5-22; no.33-37) or sterilized (no23-31). A 37th sample was obtained by cooking dried okra (no.37). Table 1 summarizes the formulations and processes undergone by each of the 37 samples. In some cases, the prepared samples were frozen a second time for the sake of convenience of the organization of the experiments.

2.1.1. Preparation of blanched okra purées

Whole fresh okras were purchased locally (Grand Frais and Paris Store, Montpellier, France). They were first steam blanched at 90°C for 7 minutes. After manual removal of seeds and stalks, the okras were ground with water (water/gumbo ratio = ¼; Stephan UMC5, Hameln, Germany, 2007). Given the foaming properties of the product, this operation was performed at 35°C at a reduced pressure of 200 mbar. The resulting purées were vacuum-packed in polyethylene bags at 100 mbar (Multivac C200, Wolfertschwenden, Germany, 2009), frozen and stored at -18°C. Before use, the purées were thawed for 1 hour at 30°C.

Two batches of blanched okra purées were prepared from 10 and 20 kg of fresh okra, independently of each other (8.1 and 7.8% dry matter and pH of 6.1 and 6.4 respectively). These blanched okra purées were then used to prepare all samples except samples 31 and 37.

2.1.2. Preparation of standardized okra purées

From the blanched okra purée, samples 1 to 4 were prepared by adjusting the water content with distilled water, and pH by adding a 20% sodium carbonate solution (table 1).

2.1.3. Preparation of cooked okra purées

From blanched okra purée, 15 samples (no.5-19) were formulated according to a three-factor Doehlert experimental design (Doehlert, 1970). The pH varied from 4 to 8 (addition of citric acid solution at 0.3 $g \cdot mL^{-1}$ or sodium carbonate solution at 20 $g \cdot mL^{-1}$), the water content from 12 to 18 $kg \cdot kg_{DM}$ (addition of distilled water) and the Ca2+ ion content from 0 to 4.8 $g_{Ca2+} \cdot kg_{DM}$ (addition of calcium chloride to 7 $g \cdot mL^{-1}$). To complete the design of experiments, 3 other formulations were also chosen (samples 20-22). After packaging in 370 mL glass jars, all these purées were then cooked at 70 or 85°C for 20 mins in a water bath and cooled in a bath of melting ice for 30 mins.

2.1.4. Preparation of sterilized okra purées

Eight Sterilized okra purées (no.23-30) were prepared in the laboratory by varying the pH, water and calcium contents in the same way as for cooked okra purées. Various sterilization treatments were tested to cover the range of sterilization values conventionally used for canned vegetables ($2.5 < F_0 <$ 10 min). After formulation, the purées were packaged in 106 mL glass jars. They were preheated in a water bath at 70 °C for 20 mins and then sterilized in an autoclave (SANOclav KL-71, Wolf, Geislingen, Germany, 1985). The core temperature of the vials was recorded every 20 s during processing using an on-board probe held in position in their geometric centre (PicoVACQ, TMI-Orion, Castelnau-le-Lez, France).

A complementary test was carried out at pilot scale on unblanched okra and that were ground with their seeds (no.31). In this case, the product was packaged in tin-plated steel cans (390 g) and sterilized in a semi-industrial autoclave (118L, Type 50, Auriol, Marmande, France, 1990). The core temperature was measured every 20 seconds with a probe placed in the geometric centre of the box. The water content of the sterilized purée was 11.3 (kg/kg dry matter), but it was readjusted according to Table 1 before rheological and textural measurements were made.

The sterilization value F0 (mins) was conventionally calculated from core temperature measurements T (°C) as a function of time t (mins) by numerical integration of the Bigelow formula.

2.1.5. Preparation of Okra sauces

Based on a traditional Cameroonian recipe for okra sauce, three samples (no.34-36) were prepared using the following ingredients: fresh okra 46.9% (w/w), water 39.4%, onions 8.4%, sunflower oil 3.5%, garlic 1.0%, salt 0.5% and 0.3% of a traditionally called "potash". This "traditional alkaline salt" is known to have an improving effect on the texture of sauces made with okra or nkui (Ngoualem, Nguimbou, & Ndjouenkeu, 2019). The "potash" used contained 170.6g/kg sodium, 42.6g/kg potassium, 14.0g/kg calcium and 4.1 g/kg magnesium and had a high alkalizing power (3.69 $meq \cdot kg^{-1}$). The whole preparation was cooked for 15 minutes at 70°C.

Two other sauces were prepared with slimy ingredients to boost the textural properties of Blanched okra purées. Sample no.32 was prepared by mixing 28% (w/w) nkui suspension, 29% water and 44% fresh okra purée. The nkui suspension used (dry matter content 1.3%) was obtained by decoction of frozen *Triumfetta pentandra* bark (JDC Africa, Paris) in boiling water for 10 mins (0.2 kg·kg-1) which was then stirred for 5 mins with a mixer equipped with a beater (RM8, Robot Coupe, Montceau-en-

Bourgogne, France) before being sieved (1mm screen). Sample no.33 was obtained by adding an ogbono suspension to blanched okra purée in the proportions (0.5 $kg \cdot kg^{-1}$). This ogbono suspension had previously been obtained from dika nut kernels (*Irvingia gabonensis*) (Merveilles d'Afrique, Paris, France), dried, ground and cooked in water for 30 mins (0.09 kg almond powder/kg water).

Finally, sample no.37 was prepared with dried okra from Mali (Ben Produits Exotiques, Paris, France). The okra was rehydrated and cooked in water at 85°C for 10 mins. Before being readjusted for rheological and textural measurements according to Table 1, the water content of the sample was 11.0 kg/kg (dry matter).

After preparation, with the exception of sample no.31, all these samples were vacuum-packaged in polyethylene bags and then, for the most part, frozen at -18°C.

For the remainder of the article, the term suspension will be used to refer to all samples (purées and sauces) used in this work.

2.2. Instrumental measurement methods

2.2.1. Physico-chemical measurements

The water content was determined by drying at 105°C for 24 hours and is expressed in kg/kg of dry matter (DM). The pH was measured using a TitroLine® 5000 pH meter (SI Analytics, Weilheim, Germany, 2017). The density of samples no.5 to 19 was evaluated by measuring the mass of a known volume of sample. Each pH, water content and density measurement was performed in triplicate.

2.2.2. Textural characterization

The operating conditions under which the Texture Analyser was used to perform penetration and stretching texture measurements are summarized in Table 2. Penetration measurements (firmness and adhesiveness) were performed in triplicate.

The experimental device used to measure the stringy nature is adapted from (Gilbert, Savary, Grisel, & Picard, 2013), and is described Figure 2. In order to avoid the test to be affected by surface heterogeneities and to guarantee the contact between the probe and the suspensions, the probe penetrated slightly inside (2 mm << depth of the steel cylinder) before stretching. After the recording of the stretching test with a camera, the software VLC media player was used to extract the image corresponding to the maximum filament breaking length prior to rupture. Then the length of the filament was measured with the software imageJ. Each measurement was repeated 15 times. The stringiness is the average of the 15 measurements.

2.2.3. Rheological characterization

The operating conditions under which the rheometer was used to perform oscillatory and steady shear measurements are summarized in Table 2. Each sample was measured 3 to 5 times with a rheometer. In order to allow a relaxation phase, the oscillatory test only started 15 minutes after the mobile was immersed in the solution. The steady shear measurement followed the oscillatory shear measurement. From the measurements made in oscillation strain sweep, the Rheoplus software was used to calculate the strain ($\gamma_{LVEG'}$) and the stress ($\sigma_{LVEG'}$) at the boundary of the Linear Viscoelastic Region (LVR), the moduli at the boundary of the LVR (LVEG', LVEG'', LVEG* and LVEtanδ), as well as the modulus G'=G'', the strain ($\gamma_{G'=G''}$) and the stress ($\sigma_{G'=G''}$) at the cross-over point. The Flow Transition Index (FTI) was calculated by dividing $\sigma_{G'=G''}$ by $\sigma_{LVEG''}$ (Corker, Ng, Poole, & García-Tuñón, 2019). From the steady shear data, the apparent viscosities at 10 s^{-1} and 100s^{-1} were determined. The Rheoplus software was used to calculate the consistency index K and the flow behavior index n using the Ostwald-de Waele equation (Eq. 2).

$$\tau = K\dot{\gamma}^n \qquad (2)$$

Where :

- τ = shear stress (Pa)
- $\dot{\gamma}$ = shear rate (s^{-1})
- K = flow consistency index ($Pa.s^n$)
- n = flow behavior index

For the remainder of the article, the term instrumental parameters will be used to refer to all variables obtained with the texturometer and the rheometer to characterize okra suspensions, which are summarized in Table 2.

2.3. Data processing and statistics

Measurements made in oscillatory shear rheology were considered valid if the measured torque was above the rheometer detection limit (50nNm). This was the case for all samples except sample no. 37, for which oscillatory shear data were not taken into account.

The data were analyzed using R-3.5.1 software (R Core Team, 2018). The coefficient of variation was the indicator used to assess the repeatability of our measurements for each parameter and sample. A Principal Component Analysis (PCA) on the 16 rheological and textural parameter and 37 samples was performed using the FactoMineR package (Lê, Josse, & Husson, 2008). A Pearson correlation matrix was produced using the corrplot package v0.84 (Wei & Simko, 2017). The other graphical representations were produced using the ggplot2 (Wickham, 2016), ggrepel (Slowikowski, 2018) and ggpubr (Kassambara, 2018) packages.

The analysis of the experimental design was performed using the rsm package (Lenth, 2009). From results of the Doehlert experimental design, correlations were established with a second-order polynomial model (Eq. 3) to determine the effects of the main formulation parameter on textural properties:

$$Y = a_0 + \sum_i a_i X_i + \sum_i a_{ii} X_i^2 + \sum_{ij} a_{ij} X_i X_j \qquad (3)$$

Where Y is the response (Consistency Index K, Flow behavior index n, Stringiness), X_i is factor i (pH, Water Content, ion calcium content), a_0 is the constant of the model, a_i is the linear effect of X_i, a_{ii} is the quadratic effect of X_i, and a_{ij} the effect of interaction between X_i and X_j.

3. RESULTS AND DISCUSSION

3.1. Rheological and textural properties of okra suspensions

The wide measurement ranges of the samples (Table 2) show that the rheological and textural properties of the samples are different from each other. It is possible to deduce some rheological properties of the analyzed okra suspensions.

3.1.1. Textural properties

From a textural point of view, okra suspensions have more or less solid properties (45 < Firmness <260 mN) and adhesive properties (60 < Adhesiveness < 690 N.m). The upper boundary of the stringiness parameter (9.4 cm measured for samples no.35 and 36) shows that some okra suspensions can have remarkable elongational properties. This is consistent with the study of the elongational properties of okra mucilage conducted by Yuan *et al.* (2018). This result also shows that it is possible to measure instrumentally the stringy properties which African consumers evaluate by hand and visually.

3.1.2. Rheological properties

The LVR of all suspensions extended to a strain of $\gamma_{LVEG'}$ = 0.1%. The interval [18%; 35%] in which the values of LVEtanδ (Table 2) are included, means that in the LVR, the suspensions have mechanical properties of viscoelastic solids, varying in magnitude depending on the samples. However, they are not real gels (LVEtanδ > 10%).

When the strain exceeds the threshold of $\gamma_{LVEG'}$ = 0.1%, the decrease in G' indicates that the material begins to deform in a non-reversible way (i.e. yield) due to the progressive but irreversible destruction of its internal structure under the effect of the strain. Some suspensions retain preponderant solid and elastic properties (G'>G'') up to very significant strains ($\gamma_{G'=G''}$ = 250%). Others are very fragile and go from solid behaviour (G'>G'') to liquid behaviour (G'<G'') at low deformations ($\gamma_{G'=G''}$ <10%).

The shear stresses required to irreversibly deform okra suspensions ($\sigma_{LVEG'}$) or cause them to flow ($\sigma_{G'=G''}$) vary from one sample to another (Table 2). Yield stress is a characteristic property of structured fluids (Nakauma, Ishihara, Funami, & Nishinari, 2011) that can be estimated with $\sigma_{G'=G''}$ (Walls, Caines, Sanchez, & Khan, 2003). The FTI is the ratio between $\sigma_{G'=G''}$ and $\sigma_{LVEG'}$ and can be used to characterize how the internal structure of the suspensions breaks. The closer the FTI is to 1, the more brittle the suspensions are (Corker *et al.*, 2019). On the opposite, the higher the FTI is, the more ductile the material is, i.e. it has the ability to deform plastically without breaking. The FTI measurement range shown in Table 2 indicates that some suspensions are not very resistant to deformation (min_{FTI} = 17) while others are very ductile (max_{FTI} = 380).

These rheological properties, which are original for sauces, are certainly linked to the existence of complex molecular structures. Observation of the curves from the oscillation strain sweep test (Figure 3) revealed that for the majority of samples (33/36 samples), at the end of the LVR, there was a slight increase in the value of G'', which is characteristic of a "weak strain overshoot" type behavior (Hyun, Kim, Ahn, & Lee, 2002). According to Hyun *et al.* (2002) and Mezger (2006), the complex structure made of polymer chains resists strain up to a certain threshold. Beyond this, the structure begins to crack and friction between the different layers causes G'' to increase. When the strain reaches a new threshold, G''' decreases as the structure breaks completely allowing the chains and/or microstructures to align in the direction of flow. This behavior would be favored by the presence of long side chains, their arrangement in space under the effect of electrostatic repulsion and the degree to which they entangle with each other to form a more or less flexible structure. In the case of okra suspensions, this explanation is plausible since it has been shown that okra pectins are of variable length and branching, with more or less long side chains (Kpodo *et al.*, 2018) and that they can entangle with each other via hydrogen, hydrophobic and calcium bonds (Ritzoulis, 2017). In fact, the samples (no.8, 10, 21, 22, 24, 30 and 34) for which the weak strain overshoot behavior is the greatest (i.e. $max_{G''/G''0}$ > 1.1) have fairly high pH values and their formulation has often been enriched with divalent cations (Table 1). Only samples n°2, 3 and 33 have a strain thinning behaviour ($max_{G''/G''0}$ = 1) which can be explained by the disentanglement of the polymer chains and their progressive alignment in the direction of flow as the strain increases (Hyun *et al.*, 2002). These differences in behavior indicate that the internal structures of the suspensions react differently to the increase in strain.

The consistency index K and the flow behavior index n are used to characterize their flow properties. The measurement ranges of parameters K and n (see Table 2) are in line with those obtained on other fruit and vegetable purées (Holdsworth, 1971). The fact that n is less than 1 for all samples means that okra suspensions have a shear thinning behavior.

These results show that different instrumental methods can be used to characterize the rheological and textural properties of okra suspensions. The next step is to identify instrumental parameters that

are necessary and sufficient to characterize and monitor the evolution of the specific rheological and textural properties of these sauces as a function of their formulation and the preservation process applied.

3.2. Repeatability of instrumental measurements

A significant proportion of samples have a coefficient of variation (CV) greater than 10% for most measurements obtained by oscillatory shear rheology (LVEG', LVEG'', LVEG*, G'=G'', $\gamma_{G'=G''}$, $\sigma_{LVEG'}$, FTI and $\sigma_{G'=G''}$, Figure 4). LVEtanδ is the only parameter obtained in dynamic rheology for which all the points have a CV < 10% and which can therefore be considered as repeatable. This low repeatability of oscillatory shear measurements comes in addition to the fact that they were not valid for one sample (no. 37).

The median CV of the stringiness measurement is about 8% (Figure 4). For 75% of the samples, it is less than 10% and less than 15% for the remaining 25%. This indicates a good level of repeatability for the stringiness measurement. For parameters measured with the texturometer (firmness, stickiness) and in steady shear rheology (K, n, η_{10} et η_{100}), the measured VC for almost all samples is less than 10% and the median CV is less than 5%. The repeatability of these 4 parameters is therefore excellent.

However, we notice that for the consistency index K, a minority of samples (samples no.2, 31 and 37) have a CV of close to 15%. For these samples, the repeatability of K is less good but remains at an acceptable level. These samples are among the most watery and have a very low consistency index K (< 30 Pa.s^n, Figure 5). These results may indicate that for the consistency index K, there is a limit of quantification below which the measurement is less repeatable and which can lie between 30 and 50 Pa.s^n. The water content alone does not fully explain the lower repeatability of the consistency index K measurements for these 3 points since sample no.32 has a CV lower than 5% while its water content is high (26.3 %).

3.3. Reduction of the number of instrumental parameters

3.3.1. Correlation of instrumental parameters with each other

In the Figure 6, it can be seen that a 2-dimensional space allows to represent 86% of the variance carried by the 16 parameters. The first dimension of the PCA (Figure 6A) is well correlated (p < 5%) with the parameters η_{10} (r = 0.99), K (r = 0.98), LVEG' (r = 0.97), LVEG* (r = 0.97), η_{100} (r = 0.97), $\sigma_{LVEG'}$ (r = 0.97), firmness (r = 0.95), $\sigma_{G'=G''}$ (0.94), n (r = -0.91), LVEG'' (r = 0.88), adhesiveness (r = 0,86) and LVEtanδ (r = -0.77). To a lesser extent, it is also correlated with the water content measurement (r = -0.50). The first component of PCR can therefore be interpreted as a dimension positively correlated with the viscous, elastic, shear thinning and adhesive properties of suspensions. The negative correlation of the water content (supplementary variable) with the first dimension illustrates this interpretation. The second dimension of the PCA is well correlated (p < 5%) with the parameters $\gamma_{G'=G''}$ (r = 0.89), G'=G'' (r = -0.78), stringiness (r = 0.75) and FTI (r = 0.68). This second dimension is therefore positively correlated with the ductility and stringy properties of suspensions. It certainly corresponds to the cohesiveness when defined as "*the extent to which a material can be deformed before it ruptures*" (Brenner *et al.*, 2014).

The meaning given to the two dimensions makes it possible to characterize the differences between the types of samples. On the first dimension of Figure 6B, the "Cooked okra purées" are clearly distinguishable (right) from the three other sample groups (left). On the second dimension, three groups of samples can be distinguished: Sterilized okra purées (bottom), Standardized okra purées and Cooked okra purées (middle) and Okra sauces (top). The study of their viscous, elastic, shear thinning and adhesive properties made it possible to distinguish two groups of suspensions, while the study of their ability to resist plastic deformation without breaking made it possible to distinguish three groups

of suspensions. Two dimensions are therefore sufficient to characterize the rheological and textural properties of slimy suspensions and necessary to differentiate them. This is consistent with the proposal of van Vliet (2002), for whom it is the combination of several parameters (viscosity, shear rate thinning behaviour and elongational flow) that would allow a good estimate of the slimy level of a solution. This result is also in line with the work of Yuan, Ritzoulis & Chen (2018) and Leakey *et al.* (2005) for whom it is the combined study of the viscous and elongational properties of okra mucilage; for the former, and of soups made with dika nut kernels; for the latter, that would best describe the original mechanical and textural properties of these slimy ingredients. Finally, in the context of research seeking to identify "gum based thickeners" with "ease of swallowing" properties, E. K. Hadde & Chen (2019) have shown the interest of jointly studying these two dimensions.

3.3.2. Identification of the parameters best correlated with the others

At the top left of the *figure 7*, a group of parameters, all correlated to each other, is clearly apparent (LVEG'', $\sigma_{LVEG'}$, LVEG', LVEG*, η_{10}, K, fimness, η_{100}, $\sigma_{G'=G''}$, adhesiveness, n and LVEtanδ). These parameters are also those that contribute significantly and strongly to the formation of the first dimension of the PCA (Figure 6A). Within this group, K and n are the two repeatable measurements (CV<10%, see Figure 4) that are best correlated with the other parameters. Indeed, the intensity correlation of K with the other parameters of this group is between 0.77 and 0.98 while the intensity correlation of n is between 0.76 and 0.88. K and n are therefore the most relevant parameters to characterize the first dimension of the PCA. From a practical point of view, it is not necessary to select one of these two parameters since they are measured at the same time and are complementary in characterizing the flow of suspensions.

At the bottom right of figure 7, the parameters $\gamma_{G'=G''}$, G'=G'', FTI and stringiness form a second group that corresponds to the second dimension of the PCA (figure 6A). Within this group, the parameters $\gamma_{G'=G''}$ and stringiness are the two parameters best correlated with the other parameters since the intensities of their correlations with the other parameters in this group are respectively between 0.52 and 0.74 and between 0.42 and 0.57. It seems more interesting to select stringiness because it is the only one of these four parameters to allow a valid measurement of sample no.37 and it has a better repeatability than $\gamma_{G'=G''}$, G'=G'' and FTI (Figure 4).

3.3.3. Comparison of the differentiating power of the consistency index K with the other parameters of the "consistency dimension"

K is very well correlated with the shear thinning (Figure 8A) and viscoelastic (Figure 8B) properties of okra suspensions as well as with their yield stress (Figure 8C) and firmness (Figure 8D). Since the flow behavior index n is less well correlated with these parameters than with K (Figure 7) and the amplitude of its measurement range is less important (Table 2), its correlations with these parameters has not been plotted in order not to multiply the graphical representations.

In the Figure 8A and Figure 8B, we observe that compared to flow behaviour index n and LVEtanδ, K makes it easier to distinguish the 4 samples (no. 7, 8, 15 and 17), for which the value of K is high (> 300 $Pa.s^n$), from the rest of the Cooked okra purées. In Figures 6C and 6D, it can be seen that K allows a better discrimination of samples with a value lower than 100 Pa.sn, than the parameters $\sigma_{G'=G''}$ and firmness. In Figures 8C and 8D, we can see that compared to $\sigma_{G'=G''}$ and firmness, K allows to better differentiate samples with a value lower than 100 $Pa.s^n$. This confirms that among the parameters of the first dimension, the consistency index K is the most suitable for differentiating samples from each other, including for high and low values of its measuring range. However, like the other parameters of the consistency dimension (Figure 6A and Figure 7), K does not allow a clear distinction between samples of the Sterilized okra purées, Standardized okra purées and Okra sauces types which have similar values.

3.3.4. Comparison of the discriminating power of stringiness with the other parameters of the "ductility-cohesiveness" dimension

As suggested by the correlation coefficients in Figure 7, it can be seen in Figure 9 that the correlations between the parameters carried by the "ductility-cohesiveness" dimension are of lower quality than for the "consistency dimension" parameters (Figure 8). This is due in particular to the presence of a few samples (No. 23, 28, 32, 35 and 36) for which the values obtained are very different from the lot.

In Figure 9A, 7/9 of Sterilized okra purées samples have a G'=G'' value similar to that of the Cooked okra purées group. Moreover, Okra sauces and Standardized okra purées samples have comparable values. In Figure 9B, the Okra sauces samples have values of $\gamma_{G'=G''}$ comparable to those of the Cooked okra purées group. In Figure 9C, except for samples 32 and 33, it is not possible to distinguish between Okra sauces, Standardized okra purées and Cooked okra purées samples using the measured FTI values. Therefore, the parameters G'=G'', $\gamma_{G'=G''}$ and FTI, shown vertically in Figures 9A, 9A and 9C, do not allow the sample groups to be correctly distinguished from each other. On the other hand, Stringiness, represented horizontally on the 3 graphs in Figure 9, makes it possible to clearly distinguish three groups of samples: Sterilized okra purées on the left, Standardized okra purées and Cooked okra purées in the centre, and Okra sauces on the right. Stringiness is therefore the parameter that best complements K since, unlike K (Figure 8), stringiness clearly distinguishes samples of the "Okra sauces", "Sterilized okra purées" and "Standardized okra purées" types.

3.3.5. Space formed by the stringiness and flow parameters to characterize the samples

The two-dimensional space formed by the combination of stringiness with K or n makes it possible to clearly distinguish the 37 suspensions that have been produced by varying the formulation and production process of the suspensions (Figure 10A and B). With the exception of sample no.37, the four types of samples form homogeneous groups and are clearly distinguishable from each other.

In Figure 10A and B, it can be seen that some samples have a similar flow properties but a very different stringiness level (see samples no.23 and no.36 for example). This result is consistent with the work of Hadde & Chen (2019) who showed that fluids could have similar properties when subjected to "shear deformation" but very different properties when subjected to "extensional deformation". In Figure 10A and B, we can see that the opposite is also true: some samples may have similar properties when subjected to "extensional deformation" but very different ones when subjected to "shear deformation" (see samples no.17 and no.30 for example). The combination of flow and stringy properties measurements is therefore suitable for discriminating slimy suspensions.

3.4. Ability of the stringiness and flow parameters to characterize the impact of the process and formulation on the textural properties of okra

3.4.1. Impact of the process on the textural properties of okra

The graphs in Figure 11 distinguish the effects of water content and process on both stringiness and suspension flow. The increase in the water content of the suspensions leads to a decrease in their consistency index K (Figure 11A) and a degradation of their shear thinning properties (increase of n in Figure 11B). However, its effect on stringiness is not obvious (Figure 11C).

Cooked okra purées and Sterilized okra purées have a similar water content (respectively between 11.9 and 17.9 and between 11.8 and 18.2 kg/kg dry matter, Table 1). Figure 11A, Figure 11B and Figure 11C show that compared to Cooked okra purées, Sterilized okra purées have a lower consistency index K, a higher flow behaviour index n and a lower stringiness level. This means that sterilization degrades the consistency, shear thinning properties and elongational properties of okra suspensions. These results confirm and supplement the researchs of Inyang & Ike (1998) and Woolfe, Chaplin, & Otchere (1977), who observed degrading effects of blanching and cooking on okra viscous properties. The

increase in LVEtanδ induced by sterilization (data not shown) reveals that heat treatment degrades the internal structure of okra suspensions. Since the degree of methylation of okra pectins is quite low (<26% according to Kpodo *et al.* (2018)), this degradation is certainly the consequence of the depolymerization of okra pectins by β-elimination or acid hydrolysis (Moelants, Cardinaels, Van Buggenhout, *et al.*, 2014).

In Figure 10, it can be seen that the sample prepared from dried okra (no.37) has very different characteristics from other Okra sauces samples but very similar to those of Sterilized okra purées. In Figure 11, we can see that compared to samples with a close water content (n°3, 16 and 31), sample n°37 is the least consistent sample and shear thinning (Figures 11A and B) and is not very stringy (Figure 11C). These results supplement those of Falade & Omojola (2010) and Inyang & Ike (1998) who showed that the drying process had an effect on the viscosity of the dried okra. It suggests that the conditions under which okra is dried in West Africa can probably be improved.

On the three charts in figure 11, it can be seen that the characteristics of the 35 and 36 samples are identical. Freezing has no impact on the stringiness and flow characteristics of okra suspensions. This confirms and supplement the results of Olorunda & Tung (1977) and Falade & Omojola (2010).

On the three charts in Figure 11, we can see that the Okra sauces to which other slimy ingredients have been added (no.32-36) have remarkable elongational properties and this for different water content levels. This means that the addition of two slimy ingredients in samples 32 and 33 increased the elongational characteristics of okra suspensions. It can be seen that the three traditional recipes (no.34 - 36) in which other ingredients, including "potash", have been added, are the most stringy. The presence of this alkaline and mineral-rich ingredient, known for its effect on okra texture (Ngoualem et al., 2019), certainly contributes to the high level of stringiness observed for these samples.

3.4.2. Impact of the formulation on the textural properties of okra

Table 3 shows that water content has a significant and dominant linear effect on all three parameters and a significant quadratic effect on K and n. The pH has a significant quadratic effect on n of the same order of magnitude as the linear effect of water content. The calcium ion content has a significant linear effect at the 15% threshold on K and n and at the 10% threshold on n but has no effect on the stringiness.

The linear effect of the water content on K (a_2 = -125.7) and n (a_2 = 0.037) indicates that the increase in water content decreases the consistency index K of the purées and their shear thinning properties. The quadratic effects of water content on K (a_{22}=67.5) and n (a_{22}=0.016) mean that these degradations are less pronounced as the water content increases. This result is in line with that of Woolfe, Chaplin & Otchere (1977) on okra mucilage. Other authors have observed similar effects of particle concentration on other plant-tissue-based suspensions (Moelants *et al.*, 2014). Increasing the water content above a certain level reduces hydrodynamic interactions between particles, which modifies the flow properties of purées (Moelants *et al.*, 2014).

The pH has a quadratic effect on the flow behavior index n (a_{11} = -0.032). Its negative sign indicates the presence of a maximum. Its intensity is of the same order of magnitude as that of the water content (a_2 = 0.037), which shows that this effect is quite significant. Woolfe, Chaplin, & Otchere (1977) showed relative viscosity of okra mucilage reaches and optimum when pH values are between 6 and 8. This could be the consequence of the effect of pH on the spatial conformation of okra pectins, which can change from a compact conformation at acidic pH to an extended one at neutral pH (Alba, Bingham, & Kontogiorgos, 2017; Alba, Kasapis, & Kontogiorgos, 2015; Ritzoulis, 2017). Furthermore, Yuan *et al.* (2018) showed that at pH4, within the okra mucilage, the particles were less numerous but larger than at pH7, and that this imparted its viscosity. Here, it is interesting to note that the pH has been shown

to have a strong and significant effect on the density of okra suspensions. At acidic pH, suspensions foamed (density < 1), which is in accordance with the emulsifying properties of okra pectins at acid pH (Alba, Ritzoulis, Georgiadis, & Kontogiorgos, 2013). All these elements indicate that by acting on the spatial conformation of okra pectins, pH modifies the properties of the matrix they form within the purées, which has an effect on their flow properties.

The calcium ion content has a negative quadratic effect (a_{33}= -0.014) on n which is dominant compared to its linear effect (a_3= 0.0052). This means that the increase in calcium ion content causes the n increase until it reaches an optimum. The other effect of the calcium ion content on the flow of the purées is to reduce their consistency index K (a_3= -13.3), which is consistent with the result of Woolfe, Chaplin, & Otchere (1977) and Ndjouenkeu *et al.* (1996). It has been suggested that by "screening" the negative charges of pectins on the surface of the particles, calcium ions facilitate the flow of purées (Moelants *et al.*, 2014). This effect is thought to have a stronger impact on their rheology than the gelling effect of Ca^{2+} ions on weakly methylated okra pectins.

The stringiness level of the purées increases linearly with their water content (a_2 = 0.8). Our results may seem contradictory to those of Yuan *et al.*, (2018) who showed that the increase in mucilage concentration resulted in an increase in break-up time (equivalent to stringiness). The difference of concentration used in the two studies (between 0.25 and 3.00% vs. between 4.9 and 7.4%) can explain this difference. In fact, additional experimental work has shown that stringy properties of okra reached a maximum at an intermediate concentration (data not shown). The relatively high concentrations used may also explain why, unlike Yuan et al. (2018), no significant pH effects on the elongational properties of okra purées were observed.

Of the three factors studied, it is the water content that has a central and dominant effect on the three parameters. But while increasing it degrades the consistency and shear thinning properties of purées, it increases their ductility. These three parameters therefore seem to measure the same phenomenon, namely the structuring or softening of the structured fluid according to its concentration of bio-polymers and particles. On the micro scale, the increase in water content reduces hydrodynamic interactions between particles and the ability of okra pectins to entangle to form a solid and elastic structure. On a macro scale, with the increase in water content, the structure becomes more flexible and its ability to resist plastic deformation without breaking increases: it becomes less fragile and more ductile. While in the experimental field studied, the stringiness of suspensions is only sensitive to water content, their flow properties are also sensitive to calcium ion concentration and pH. As we have shown that the stringiness parameter has a better ability than the flow parameters to differentiate between sample types, this confirms that it useful to keep all three parameters to study the impact of the process and formulation on the rheology and texture of okra suspensions.

4. CONCLUSION

Sixteen rheological and textural parameters were measured to characterize the texture and rheology of okra slimy suspensions. These suspensions have viscoelastic, shear thinning, adhesive, stringy, ductile and cohesive properties, and can be classified as structured fluids. A PCA showed that two dimensions are sufficient to characterize their rheological and textural properties and necessary to differentiate them. While the first dimension is correlated with their viscoelastic, shear thinning and adhesive properties, the second dimension is correlated with their stringy, cohesive and ductile properties. Consistency index K and flow behavior index n are two repeatable measures that are very well correlated with the other 10 parameters carried by the first dimension of the PCA. Stringiness is a repeatable measurement that is well correlated with the other 3 parameters of the second dimension ($\gamma_{G'=G''}$, G'=G'' and FTI).

Combining the consistency index K and the stringiness is very good at differentiating the samples with respect to the process and the formulation they have undergone. These instrumental parameters therefore seem complementary in their ability to i) characterize the degree of structure of the slimy suspensions as a function of their formulation and ii) monitor the degradation of their rheological and textural properties as a result of the process. This work therefore makes it possible to find levers to limit the degradation of the rheological and textural properties of okra during processing. To this end, it would be helpful to study which biochemical mechanisms are involved in these degradations.

The fact that slimy sauces, like other slimy solutions such as hagfish slime (Böni, Fischer, Böcker, Kuster, & Rühs, 2016), have remarkable stringy properties suggests that this characteristic could be related to the sensory perception of the slimy texture. An adapted sensory analysis work will have to be carried out in order to validate the existence of such a correlation. If this is confirmed, it will be possible to use the set of measuring methods identified in this work to engineer the texture and the rheology of African slimy sauces.

ACKNOWLEDGMENTS

We would like to express our thanks to Mr. and Mrs. Nono (AS Food International) for their support and expertise in the production of traditional okra sauce preparation as well as Nourdène Dhaouadi, an engineering student from Montpellier SupAgro, for her contribution to the experiments.

ETHICAL STATEMENTS

The authors declare that they do not have any conflict of interest

REFERENCES

Alba, K., Bingham, R. J., & Kontogiorgos, V. (2017). Mesoscopic structure of pectin in solution: *Biopolymers*, *107*, 1–8. doi:10.1002/bip.23016

Alba, K., Kasapis, S., & Kontogiorgos, V. (2015). Influence of pH on mechanical relaxations in high solids LM-pectin preparations. *Carbohydrate Polymers, 127,* 182–188. doi:10.1016/j.carbpol.2015.03.051

Alba, K., Ritzoulis, C., Georgiadis, N., & Kontogiorgos, V. (2013). Okra extracts as emulsifiers for acidic emulsions. *Food Research International*, 54, 1730–1737. doi:10.1016/j.foodres.2013.09.051

Böni, L., Fischer, P., Böcker, L., Kuster, S., & Rühs, P. A. (2016). Hagfish slime and mucin flow properties and their implications for defense. *Scientific Reports*, *6*, 1–8. doi:10.1038/srep30371

Bourne, M. C. (2002). *Food texture and viscosity: Concept and measurement* (2nd ed). San Diego: Academic Press.

Brenner, T., Hayakawa, F., Ishihara, S., Tanaka, Y., Nakauma, M., Kohyama, K., … Nishinari, K. (2014). Linear and Nonlinear Rheology of Mixed Polysaccharide Gels. Pt. II. Extrusion, Compression, Puncture and Extension Tests and Correlation with Sensory Evaluation. *Journal of Texture Studies*, *45*, 30–46. doi:10.1111/jtxs.12049

Corker, A., Ng, H. C.-H., Poole, R. J., & García-Tuñón, E. (2019). 3D printing with 2D colloids: Designing rheology protocols to predict 'printability' of soft-materials. *Soft Matter*, *15*, 1444–1456. doi:10.1039/C8SM01936C

Doehlert, D. H. (1970). Uniform Shell Designs. *Journal of the Royal Statistical Society. Series C (Applied Statistics)*, *19*, 231–239. doi:10.2307/2346327

Falade, K. O., & Omojola, B. S. (2010). Effect of Processing Methods on Physical, Chemical, Rheological, and Sensory Properties of Okra (*Abelmoschus esculentus*). *Food and Bioprocess Technology*, *3*, 387–394. doi:10.1007/s11947-008-0126-2

Fasogbon, B. M., Taiwo, K. A., & Adeniran, H. A. (2017). Sensory profiling of ogbono soup mix and its nutritional characterisation. *Annals of Food Science and Technology*, *18*, 552–563.

Gilbert, L., Savary, G., Grisel, M., & Picard, C. (2013). Predicting sensory texture properties of cosmetic emulsions by physical measurements. *Chemometrics and Intelligent Laboratory Systems*, *124*, 21–31. doi:10.1016/j.chemolab.2013.03.002

Hadde, E. K., & Chen, J. (2019). Shear and extensional rheological characterization of thickened fluid for dysphagia management. *Journal of Food Engineering*, *245*, 18–23. doi:10.1016/j.jfoodeng.2018.10.007

Holdsworth, S. D. (1971). Applicability of Rheological Models to the Interpretation of Flow and Processing Behaviour of Fluid Food Products. *Journal of Texture Studies*, *2*, 393–418. doi:10.1111/j.1745-4603.1971.tb00589.x

Hyun, K., Kim, S. H., Ahn, K. H., & Lee, S. J. (2002). Large amplitude oscillatory shear as a way to classify the complex fluids. *Journal of Non-Newtonian Fluid Mechanics*, *107*, 51–65. doi:10.1016/S0377-0257(02)00141-6

Inyang, U. E., & Ike, C. I. (1998). Effect of blanching, dehydration method and temperature on the ascorbic acid, colour, sliminess and other constituents of okra fruit. *International Journal of Food Sciences and Nutrition*, 49, 125–130. doi:10.3109/09637489809089392

Kassambara, A. (2018). ggpubr: "ggplot2" Based Publication Ready Plots (Version 0.2). Retrieved from https://CRAN.R-project.org/package=ggpubr

Kontogiorgos, V., Margelou, I., Georgiadis, N., & Ritzoulis, C. (2012). Rheological characterization of okra pectins. *Food Hydrocolloids,* 29, 356–362. doi:10.1016/j.foodhyd.2012.04.003

Kouebou, C. P., Achu, M., Nzali, S., Chelea, M., Bonglaisin, J., Kamda, A., … Kana Sop, M. M. (2013). A review of composition studies of Cameroon traditional dishes: Macronutrients and minerals. *Food Chemistry*, *140*, 483–494. doi:10.1016/j.foodchem.2013.01.003

Kpodo, F. M., Agbenorhevi, J. K., Alba, K., Oduro, I. N., Morris, G. A., & Kontogiorgos, V. (2018). Structure-Function Relationships in Pectin Emulsification. *Food Biophysics*. doi:10.1007/s11483-017-9513-4

Lê, S., Josse, J., & Husson, F. (2008). FactoMineR: A Package for Multivariate Analysis. *Journal of Statistical Software*, *25*, 1–18. https://doi.org/10.18637/jss.v025.i01

Leakey, R. R. B., Greenwell, P., Hall, M. N., Atangana, A. R., Usoro, C., Anegbeh, P. O., … Tchoundjeu, Z. (2005). Domestication of *Irvingia gabonensis*: 4. Tree-to-tree variation in food-thickening properties and in fat and protein contents of dika nut. *Food Chemistry*, *90*, 365–378. doi:10.1016/j.foodchem.2004.04.012

Lenth, R. V. (2009). Response-Surface Methods in *R*, Using rsm. *Journal of Statistical Software*, *32*(7), 1–17. doi:10.18637/jss.v032.i07

Mateus-Reguengo, L., Barbosa-Pereira, L., Rembangouet, W., Bertolino, M., Giordano, M., Rojo-Poveda, O., & Zeppa, G. (2019). Food applications of *Irvingia gabonensis* (Aubry-Lecomte ex. O'Rorke) Baill., the 'bush mango': A review. *Critical Reviews in Food Science and Nutrition*, 1–14. doi:10.1080/10408398.2019.1646704

Mezger, T. G. (2006). *The Rheology Handbook* (2nd ed.). Hannover: Vincentz Network GmbH & Co.

Moelants, K. R. N., Cardinaels, R., Van Buggenhout, S., Van Loey, A. M., Moldenaers, P., & Hendrickx, M. E. (2014). A Review on the Relationships between Processing, Food Structure, and Rheological Properties of Plant-Tissue-Based Food Suspensions. *Comprehensive Reviews in Food Science and Food Safety*, *13*, 241–260. doi:10.1111/1541-4337.12059

Nakauma, M., Ishihara, S., Funami, T., & Nishinari, K. (2011). Swallowing profiles of food polysaccharide solutions with different flow behaviors. *Food Hydrocolloids*, *25*, 1165–1173. doi:10.1016/j.foodhyd.2010.11.003

Ndjouenkeu, R., Goycoolea, F. M., Morris, E. R., & Akingbala, J. O. (1996). Rheology of okra (*Hibiscus esculentus* L.) and dika nut (*Irvingia gabonensis*) polysaccharides. *Carbohydrate Polymers, 29*, 263–269 doi:10.1016/0144-8617(96)00016-1

Ngoualem, F. K., Nguimbou, R. M., & Ndjouenkeu, R. (2019). Variability and Functionalities of Salts Used in Traditional African Food Preparations. *Journal of Scientific Research and Reports*, *24*, 1–14. doi:10.9734/jsrr/2019/v24i330154

Nishinari, K., Fang, Y., & Rosenthal, A. (2019). Human oral processing and texture profile analysis parameters: Bridging the gap between the sensory evaluation and the instrumental measurements. *Journal of Texture Studies*, 50, 369-380. doi:10.1111/jtxs.12404

Olorunda, A. O., & Tung, M. A. (1977). Rheology of fresh and frozen okra dispersions. *International Journal of Food Science & Technology*, *12*, 593–598. doi:10.1111/j.1365-2621.1977.tb00145.x

Owoeye, A. I., Caurie, M. C., Allagheny, N. N., & Onyezili, F. N. (1990). Chemical and physical parameters affecting the viscosity of mixed okra and tomato homogenate. *Journal of the Science of Food and Agriculture*, *53*, 283–286. doi:10.1002/jsfa.2740530218

R Core Team. (2018). R: A language and environment for statistical computing (Version R-3.5.1). Retrieved from https://www.R-project.org/

Richardson, R. K., Morris, E. R., Ross-Murphy, S. B., Taylor, L. J., & Dea, I. C. (1989). Characterization of the perceived texture of thickened systems by dynamic viscosity measurements. *Food Hydrocolloids*, *3*, 175–191. doi:10.1016/S0268-005X(89)80002-5

Ritzoulis, C. (2017). Mucilage formation in food: A review on the example of okra. *International Journal of Food Science & Technology*, *52*, 59–67. doi:10.1111/ijfs.13270

Rosenthal, A. J. (2010). Texture Profile Analysis – How important are the parameters? *Journal of Texture Studies*, *41*, 672–684. https://doi.org/10.1111/j.1745-4603.2010.00248.x

Sengkhamparn, N., Sagis, L. M. C., De Vries, R., Schols, H. A., Sajjaanantakul, T., & Voragen, A. G. J. (2010). Physicochemical properties of pectins from okra (Abelmoschus esculentus (L.) Moench). *Food Hydrocolloids, 24*, 35–41. doi: 10.1016/j.foodhyd.2009.07.007

Sharma, M., Kristo, E., Corredig, M., & Duizer, L. (2017). Effect of hydrocolloid type on texture of pureed carrots: Rheological and sensory measures. *Food Hydrocolloids*, *63*, 478–487. https://doi.org/10.1016/j.foodhyd.2016.09.040

Slowikowski, K. (2018). ggrepel: Automatically Position Non-Overlapping Text Labels with “ggplot2” (Version 0.8.0). Retrieved from https://CRAN.R-project.org/package=ggrepel

Szczesniak, A. S., & Farkas, E. (1962). Objective characterization of the mouthfeel of gum solutions. *Journal of Food Science*, *27*, 381–385. doi:10.1111/j.1365-2621.1962.tb00112.x

Terpstra, M. E. J., Jellema, R. H., Janssen, A. M., Wijk, R. a. D., Prinz, J. F., & Linden, E. V. D. (2009). Prediction of Texture Perception of Mayonnaises from Rheological and Novel Instrumental Measurements. *Journal of Texture Studies*, *40*, 82–108. doi:10.1111/j.1745-4603.2008.00171.x

Uzo, J. O., & Ojiako, G. U. (1980). A Physical Method for Measuring Okra Fruit Quality. *Journal of Food Science*, *45*, 390–391. doi:10.1111/j.1365-2621.1980.tb02623.x

Van Vliet, T. (2002). On the relation between texture perception and fundamental mechanical parameters for liquids and time dependent solids. *Food Quality and Preference*, *13*, 227–236. doi:10.1016/S0950-3293(01)00044-1

Walls, H. J., Caines, S. B., Sanchez, A. M., & Khan, S. A. (2003). Yield stress and wall slip phenomena in colloidal silica gels. *Journal of Rheology*, *47*, 847–868. doi:10.1122/1.1574023

Wei, T., & Simko, V. (2017). R package “corrplot”: Visualization of a Correlation Matrix (Version 0.84). Retrieved from https://github.com/taiyun/corrplot

Wickham, H. (2016). *ggplot2: Elegant Graphics for Data Analysis*. Retrieved from http://ggplot2.org

Wood, F. W. (1974). An approach to understanding creaminess. *Starch-Stärke*, *26*, 127–130. doi: pdf/10.1002/star.19740260406

Woolfe, M. L., Chaplin, M. F., & Otchere, G. (1977). Studies on the mucilages extracted from okra fruits (*Hibiscus esculentus* L.) and baobab leaves (*Adansonia digitata* L.). *Journal of the Science of Food and Agriculture*, *28*, 519–529. doi:10.1002/jsfa.2740280609

Yuan, B., Ritzoulis, C., & Chen, J. (2018). Extensional and shear rheology of a food hydrocolloid. *Food Hydrocolloids*, *74*, 296–306. doi:10.1016/j.foodhyd.2017.08.019

641 Tables legends

642 Table 1. Summary of main preparation process and formulation of the 37 samples used for rheological
643 and textural analysis

644 Table 2. Instrumental methods and parameters selected for characterizing rheological and textural
645 properties of okra suspensions

646 Table 3. Effects of pH, water content and calcium ion content on the consistency index K, the flow
647 behavior index n and the stringiness of cooked okra purées (samples n°5-19)

648

649

650

651

652 Table 1 : Summary of main preparation process and formulation of the 37 samples used for
653 rheological and textural analysis

Sample Number	Name		pH	Water content (kg/kg dry matter)	Added calcium (g Ca^{2+}/kg dry matter)	Thermal process Temperature (°C) x time (min) [F_0 for sterilization (min)]
1	Standardized okra purées		7.2	15.8	0	
2			7.3	25.3	0	
3			6.4	19.0	0	
4			7.1	19.5	0	
5	Cooked okra purées		6.0	14.9	2.4	70 x 20
6			6.0	16.4	2.4	
7			4.5	11.9	2.4	
8			7.1	12.2	2.4	
9			4.6	17.2	2.4	
10			7.4	16.5	2.4	
11			4.6	14.5	0.7	
12			7.4	14.8	0.7	
13			4.6	14.9	4.1	
14			7.4	14.6	4.1	
15			6.0	12.2	0.7	
16			6.1	17.9	0.7	
17			6.0	12.0	4.1	
18			6.0	17.1	4.1	
19			6.0	14.6	2.4	
20			6.2	15.9	0	
21			7.2	15.1	4.8	
22			7.3	15.0	4.8	85 x 19
23	Sterilized okra purées		5.2	15.4	0	115 x 58 [F_0 = 5.4]
24			5.9	16.3	0	125 x 22 [F_0 = 3.4]
25			5.4	15.9	0	125 x 26 [F_0 = 7.3]
26			5.7	15.8	0	120 x 35 [F_0 = 6.7]
27			5.5	16.2	0	120 x 50 [F_0 = 9.9]
28			4.3	12.6	3	125 x 24 [F_0 = 7.5]
29			7.6	11.8	4.8	125 x 24 [F_0 = 8.1]
30			6.4	15.3	4.8	125 x 21 [F_0 = 5.6]
31			5.7	18.2	0	121 x 60 [F_0 = 4.2]
32	Okra sauces†	With Nkui	6.6	26.3	0	
33		With Ogbono	5.8	10.1	0	80 x 30
34		Traditional recipe 1	7.7	7.1	0	70 x 15
35		Traditional recipe 2	6.5	8.8	0	70 x 15
36		Frozen traditional recipe 2	6.5	8.8	0	70 x 15
37		Dried okra sauce	6.3	18.5	0	85 x 20

†: See section 2.1.5. for further explanations about Okra sauce formulation and preparation.

654 Table 2 : Instrumental methods and parameters selected for characterizing rheological and textural
655 properties of okra suspensions

656

Methods					Value range obtained with the 37 samples
Material	**Type of measurement**	**Selected parameter**	**Description**	**References**	
Anton Paar MCR 301 rheometer equipped with the starch cell C-ETD160/ST and with the measuring geometry ST24-2D/2V/2V-30 (stirrer with 3 pairs of blades)	**Oscillation strain sweep test:** frequency = 1 Hz; strain interval = [0.001; 1000] %; 5 measurement/strain decade; temperature = 25°C	LVEG'	Elastic modulus at the end of the Linear Viscoelastic Region	Mezger (2006) & Walls, Caines, Sanchez, & Khan (2003)	[100; 7410] Pa
		LVEG''	Viscous modulus at the end of the Linear Viscoelastic Region		[30; 1500] Pa
		LVEG*	Complex modulus at the end of the Linear Viscoelastic Region		[100; 7540] Pa
		LVEtanδ	Damping factor at the end of the Linear Viscoelastic Region		[18; 35] %
		$\gamma_{LVEG'}$	Strain at LVEG' (limit of the Linear Viscoelastic Region)		0,10%
		$\sigma_{LVEG'}$	Stress at LVEG'		[0.1 ; 7.5] Pa
		G'=G''	Modulus at cross-over point		[10; 940] Pa
		$\sigma_{G'=G''}$	Stress at cross-over point		[13; 470] Pa
		$\gamma_{G'=G''}$	Strain at cross-over point		[6; 250] %
		FTI	Flow Transition Index = $\sigma_{G'=G''}/\sigma_{LVEG'}$	Corker, Ng, Poole, & García-Tuñón (2019)	[17; 380]
	Flow measurement under steady state : shear rate interval = [0.001; 1000] s^{-1}; 5 measurement/shear rate decade; temperature = 25°C	K	Consistency index K calculated using the de Waele-Ostwald equation	Mezger (2006), Holdsworth (1971)	[3; 340] $Pa.s^n$
		n	Flow behavior index calculated using the de Waele-Ostwald equation		[0.16; 0.66]
		η_{10}	Apparent viscosity measured at 10 s^{-1}	Sharma, Kristo, Corredig, & Duizer (2017)	[2; 50] Pa.s
		η_{100}	Apparent viscosity measured at 100 s^{-1}		[0.6; 6] Pa.s

Stable Micro Systems TA.XT.plus Texture Analyser equipped with the same PVC cylindrical probe (diameter = 2 cm)	**Penetration**: The sauce was poured and tossed in a glass beaker (depth = 3 cm; diameter = 6 cm). The sample was left to relax for 2 min, before a single compression test was performed with following settings: Pre-test, test and post-test speed = 2 mm.s^{-1}; trigger force = 3 g; penetration distance = 3 mm. Temperature = 25°C (±1°C)	Firmness	Maximum force measured at the end of the penetration into the product	Nishinari et al. (2019), Rosenthal (2010), Bourne (2002)	[45; 260] mN
		Adhesiveness	Area under the curve force corresponding to the work of adhesiveness while the probe is pulling up back from the sauce		[60; 690] N.m
	Stretching: The sauce was poured and tossed in a steel cylinder (diameter = 3 cm). The sample was let to relax for 2 min before that a single compression test was performed with following settings: Pre-test speed = 10 mm.s^{-1}, test and post-test speed = 40 mms.s^{-1}; trigger force = 2 g; penetration distance = 2 mm. Temperature = 25°C (±1°C)	Stringiness	Average breaking length of the filament	Gilbert et al. (2013)	[1.2; 9.4] cm

657

658 Table 3: Effects of pH, water content and calcium ion content on the consistency index K, the flow
659 behavior index n and the stringiness of cooked okra purées (samples n°5-19)

Coefficient†	Consistency index K ($Pa.s^n$)	Flow behaviour index n	Stringiness
Constant			
a_0	203.9*****	0.216*****	3.8*****
Linear			
a_1	4.6	0.005	0.0
a_2	-125.7*****	0.037*****	0.8*****
a_3	-13.3*	0.0052*	0.1
Interactions			
a_{12}	-14.8	-0.001	-0.2
a_{13}	19.1	0.008	-0.2
a_{23}	-0.5	-0.005	0.0
Quadratic			
a_{11}	-3.4	-0.032****	-0.2
a_{22}	67.5****	-0.016**	0.0
a_{33}	4.4	-0.014**	-0.1
R^2	0.9817	0.9712	0.9539
† Indices 1, 2, and 3 refer to pH, Water Content, and Calcium ion content respectively. Significance (p-value) : ***** <0.01% / **** <1% /*** <5% / **<10% / *<15%			

660

661

Figures legends

Figure 1: Production diagram of the 37 samples used for rheological and textural analyses.

Figure 2: Drawing of the experimental set-up for stringiness measuring

Figure 3: Elastic (G') and Viscous (G'') moduli of the 36 samples (measurements of the sample no.37 were not valid) as a function of strain at 1Hz (A and B). Reduced moduli G'/G'_0 and G''/G''_0 versus strain, where G'0 and G''0 are the moduli measured at the beginning of the linear viscoelastic region (see (Hyun et al., 2002)).

Figure 4: Distribution of coefficient of variation (CV) measured on the 37 samples for the 16 rheological and textural parameters. The numbers indicate the samples for which an extreme CV has been measured. The 10% dashed line corresponds to the threshold above which the measurement was not considered repeatable.

Figure 5: Variation coefficient of consistency index K vs measured consistency index K. The color gradient of the points corresponds to the water content (dry matter) of the measured samples. The sample number is written when the measured value is less than 50 $Pa.s^n$. The 10% dashed line corresponds to the threshold above which the measurement was not considered repeatable.

Figure 6: Principal Component Analysis (PCA) biplot of the 16 textural and rheological parameters and the 36 samples. The explained variance for PC1 and PC2 is 66.61 % and 19.68 %. On the parameters factor map (A), Water Content is a supplementary parameter that does not contribute to the formation of the components. On the Projection of individuals (B), the number indicates samples and confidence ellipses were traced around the samples categories.

Figure 7: Pearson correlation coefficients matrix of the 16 parameters. The lower left half shows the Pearson correlation coefficients significant at the 5% threshold. The upper right half shows the graphical representation of these coefficients: their color depends on the sign of the correlation while the size of the disks and the intensity of the color represent the intensity of the correlation.

Figure 8: Graphical illustrations of the correlation between the consistency index K and the main rheological and textural properties of the first dimension of the PCA: flow behavior index n (A), LVEtanδ (B), $\sigma_{G'=G''}$ (C) and firmness (D).

Figure 9: Graphical illustrations of the correlation between stringiness and the main rheological and textural properties of the second dimension of the PCA: $\gamma_{G'=G''}$ (A), G'=G'' (B), FTI (C).

Figure 10: The two-dimensional space formed by stringiness in combination with the consistency index K (A) and the flow behavior index n (B).

Figure 11: Water-dependence of flow consistency index K (A), flow behaviour index n (B) and stringiness (C) for the 37 suspensions.

701 Figure 1: Production diagram of the 37 samples used for rheological and textural analyses.

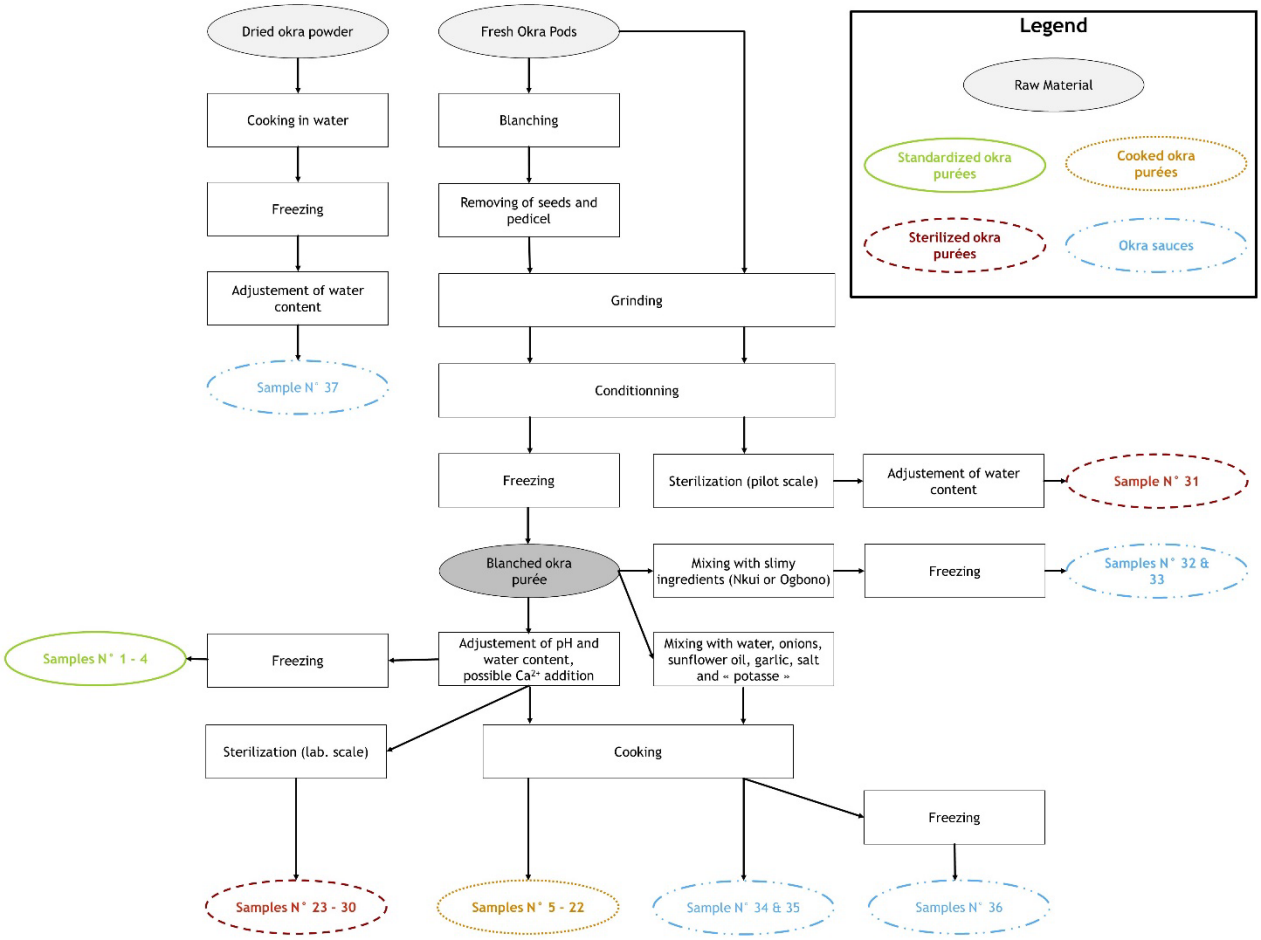

702

703 Figure 2: Drawing of the experimental set-up for measuring the stringiness

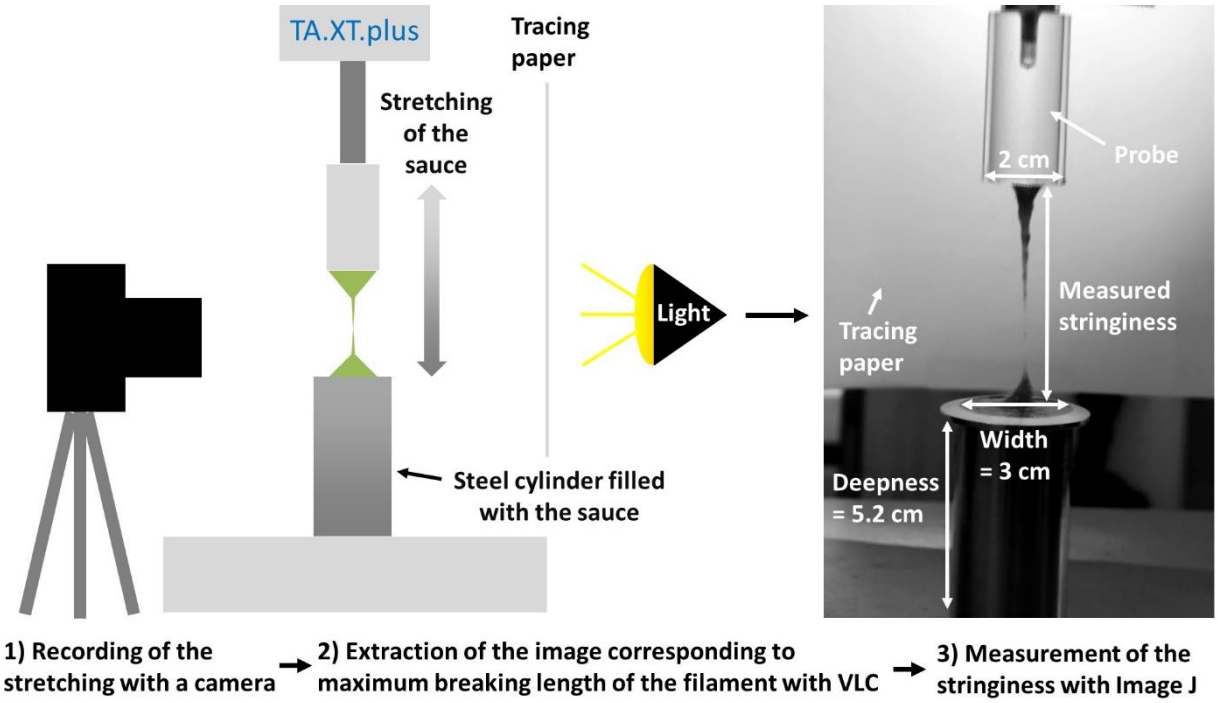

704

705

706

707 Figure 3: Elastic (G') and Viscous (G'') moduli of the 36 samples (measurements of the sample n°37
708 were not valid) as a function of strain at 1Hz (A and B). Reduced moduli G'/G'_0 and G''/G''_0 versus
709 strain, where G'0 and G''0 are the moduli measured at the beginning of the linear viscoelastic region
710 (see (Hyun et al. 2002)).

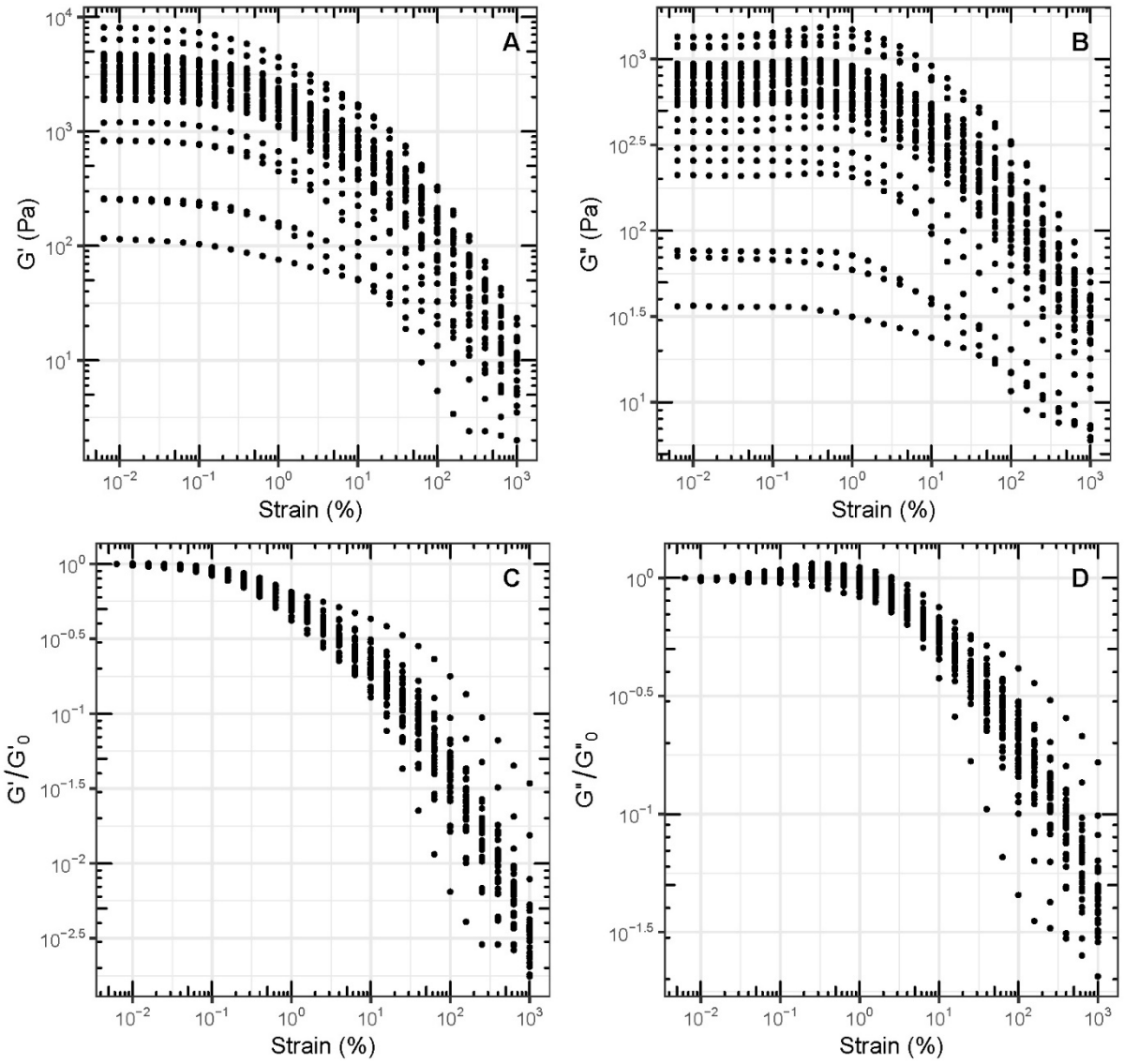

711

712

713

Figure 4: Distribution of Variation Coefficients (CV) measured on the 37 samples for the 16 rheological and textural parameters. The numbers indicate the samples for which an extreme CV has been measured. The 10% dash line corresponds to the threshold above which the measurement was not considered repeatable.

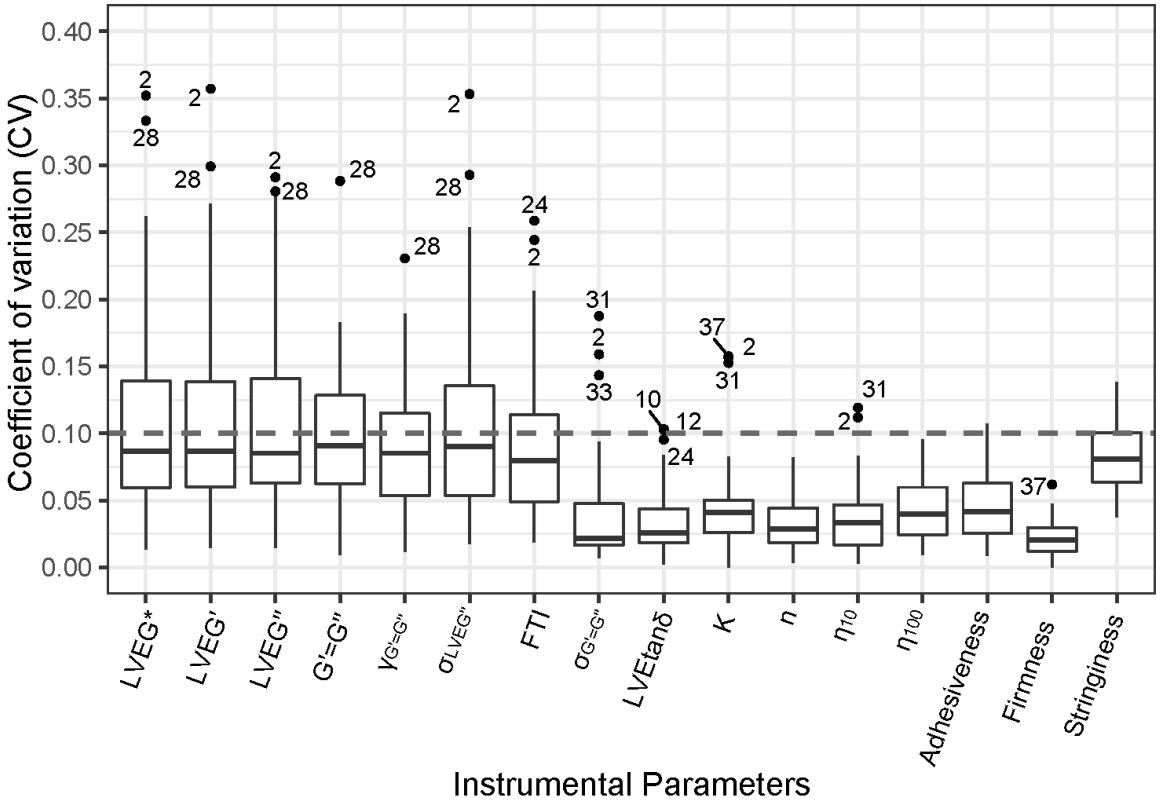

720 Figure 5: Variation coefficient of consistency index K vs measured consistency index K. The color
721 gradient of point corresponds to the water content (dry matter) of the measured samples. The
722 sample number is written when the measured value is less than *50 Pa.sn.*

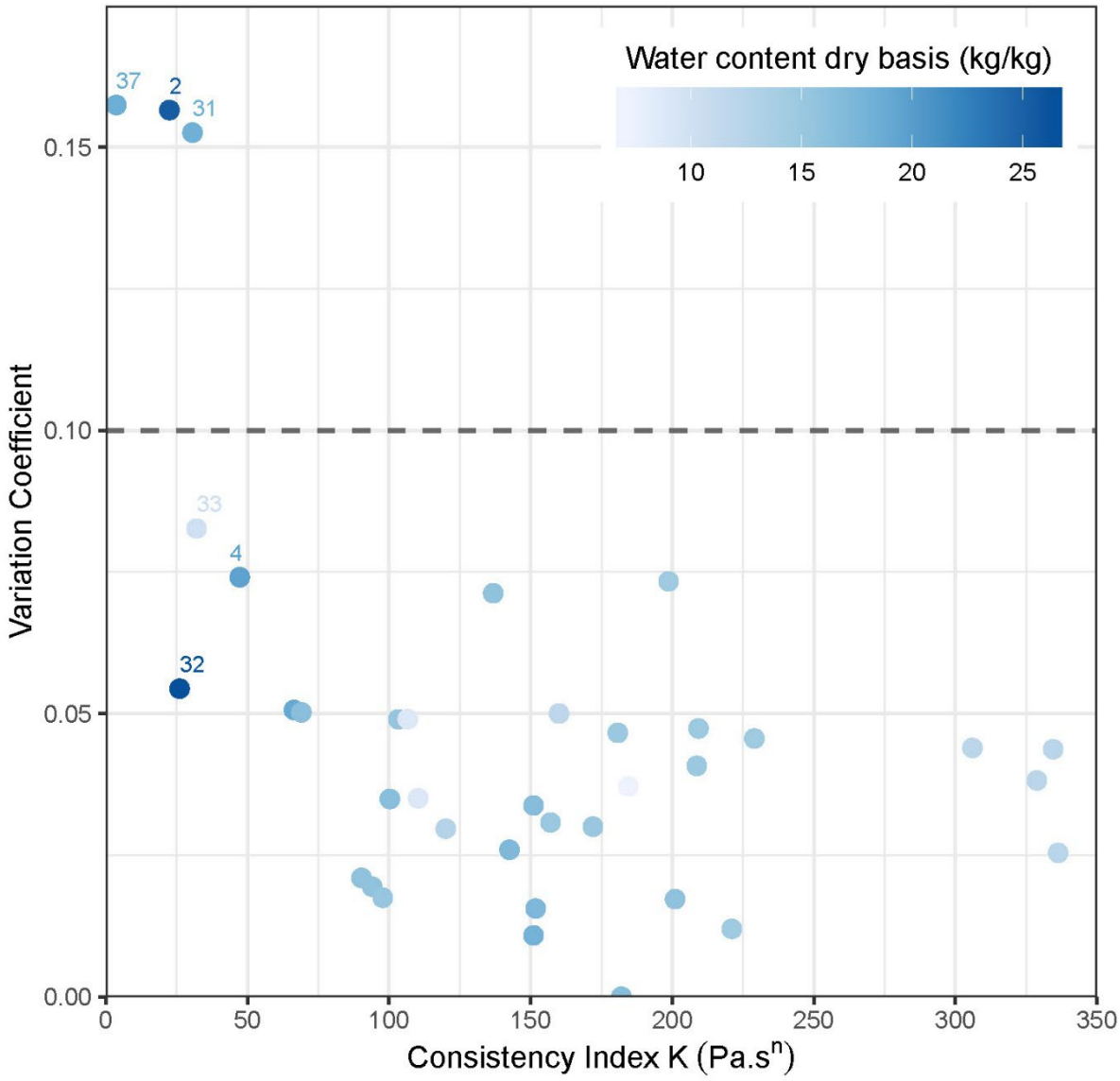

723

724

725

726

727 Figure 6: Principal Component Analysis (PCA) biplot of the 16 textural and rheological parameters
728 and the 36 samples. The explained variance for PC1 and PC2 is 66.61 % and 19.68 %. On the
729 parameters factor map (A), Water Content is a supplementary parameter that does not contribute to
730 the formation of the components. On the Projection of individuals (B), the number indicates samples
731 and confidence ellipses were traced around the samples

732

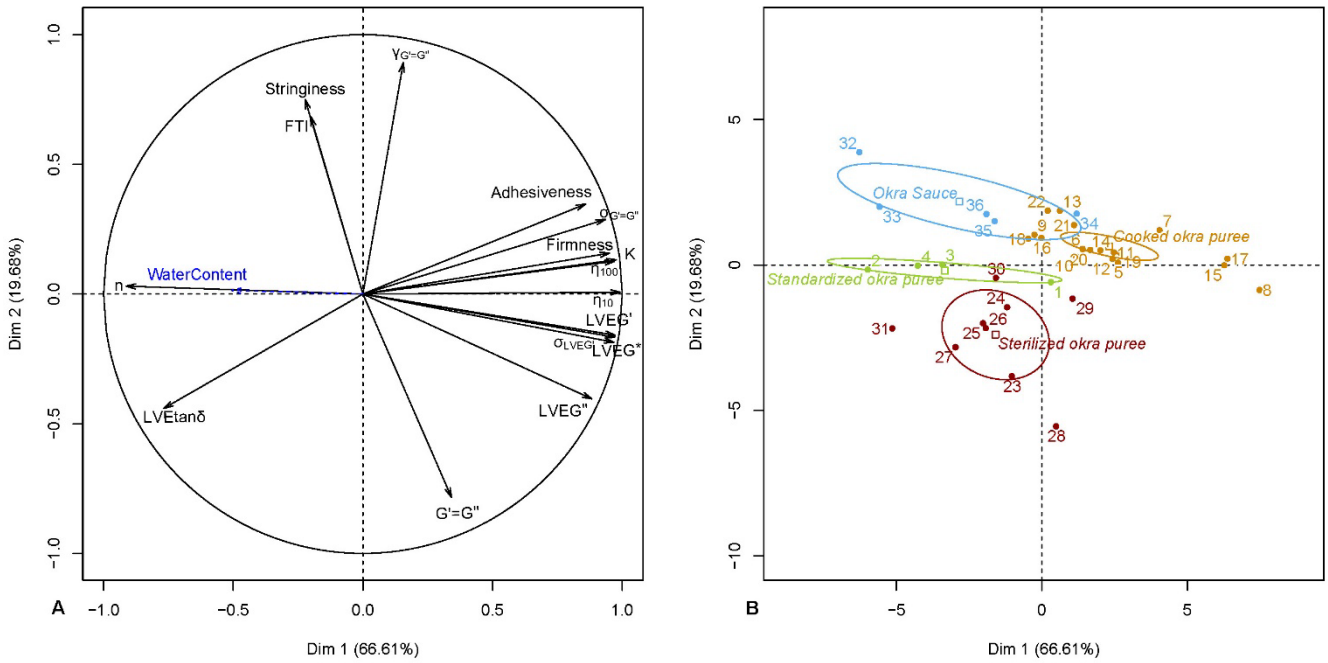

733

Figure 7: Pearson correlation coefficients matrix of the 16 parameters. The lower left half shows the Pearson correlation coefficients significant at the 5% threshold. The upper right half shows the graphical representation of these coefficients: their color depends on the sign of the correlation while the size of the disks and the intensity of the color represent the intensity of the correlation.

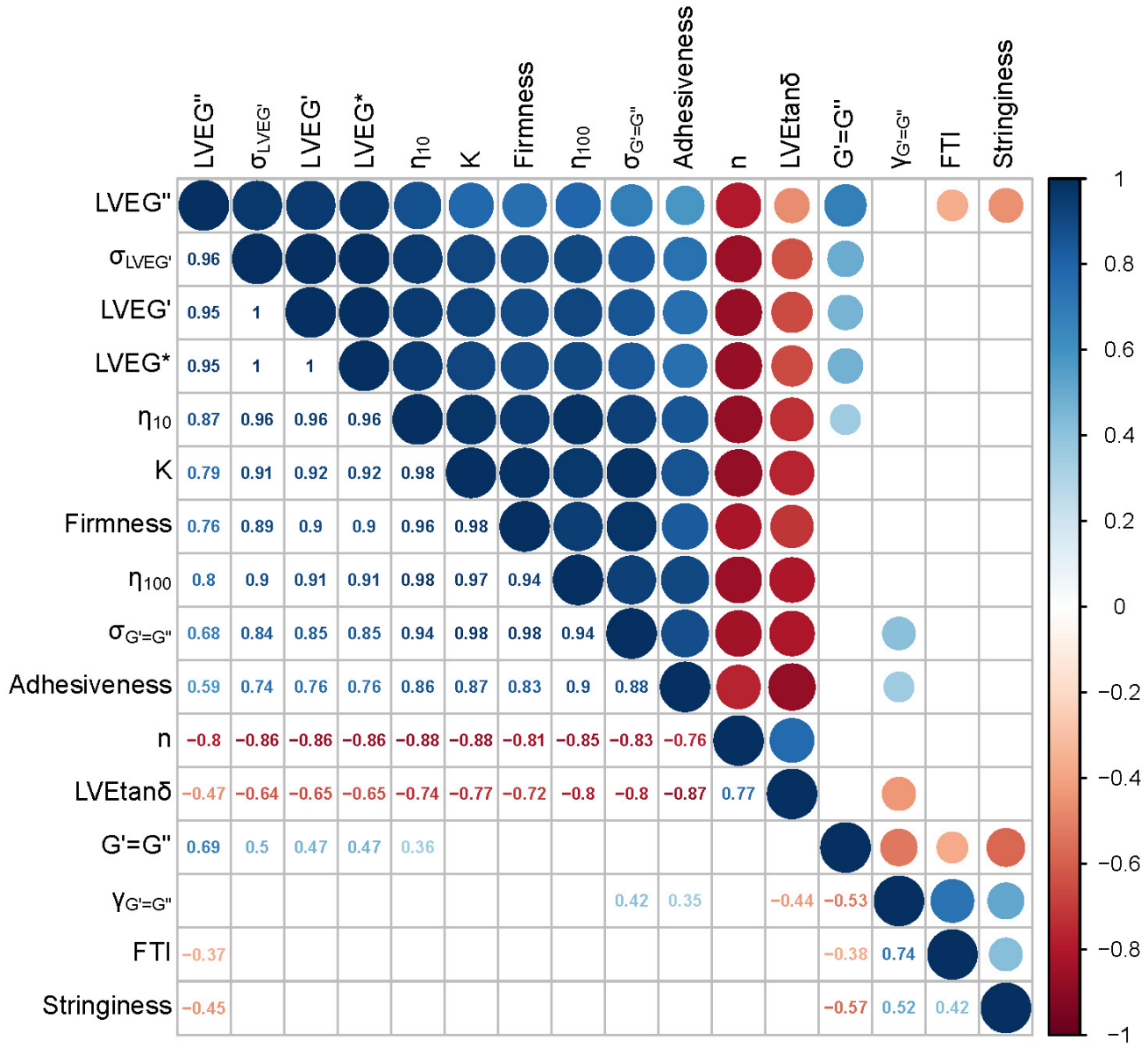

743 Figure 8: Graphical illustrations of the correlation between the consistency index K and the main
744 rheological and textural properties of the first dimension of the PCA: flow behavior index n (A),
745 LVEtanδ (B), $\sigma_{G'=G''}$ (CD) and firmness (D).

746

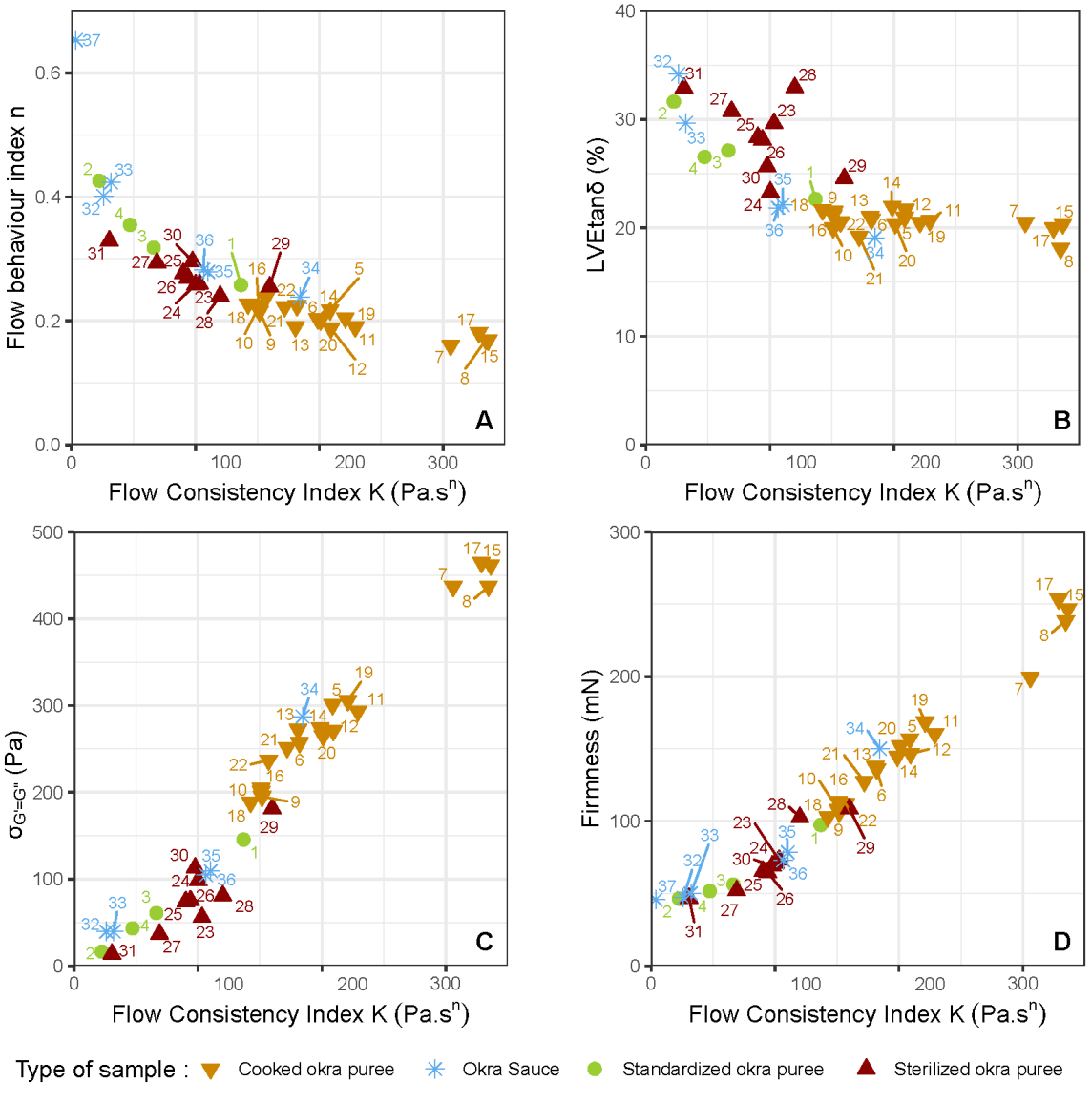

747

748

749 Figure 9: Graphical illustrations of the correlation between stringiness and the main rheological and
750 textural properties of the second dimension of the PCA: $\gamma_{G'=G''}$ (A), G'=G'' (B), FTI (C).

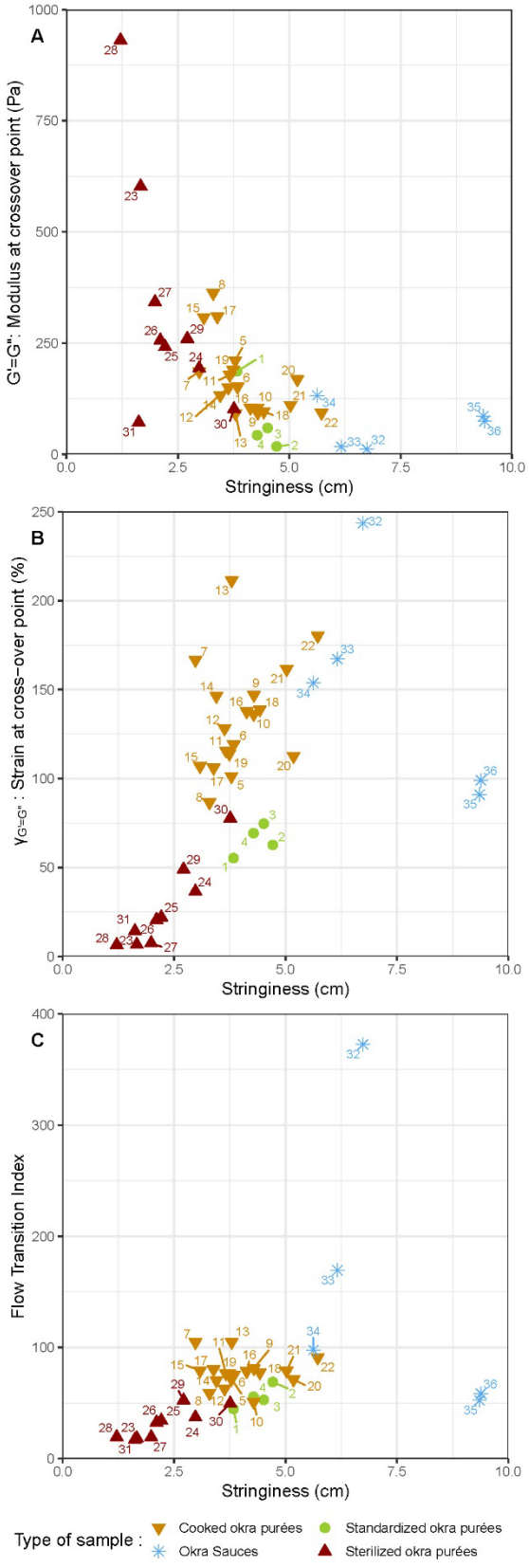

751

752 Figure 10: The two-dimensional space formed by stringiness in combination with the consistency
753 index K (A) and the flow behavior index n (B).

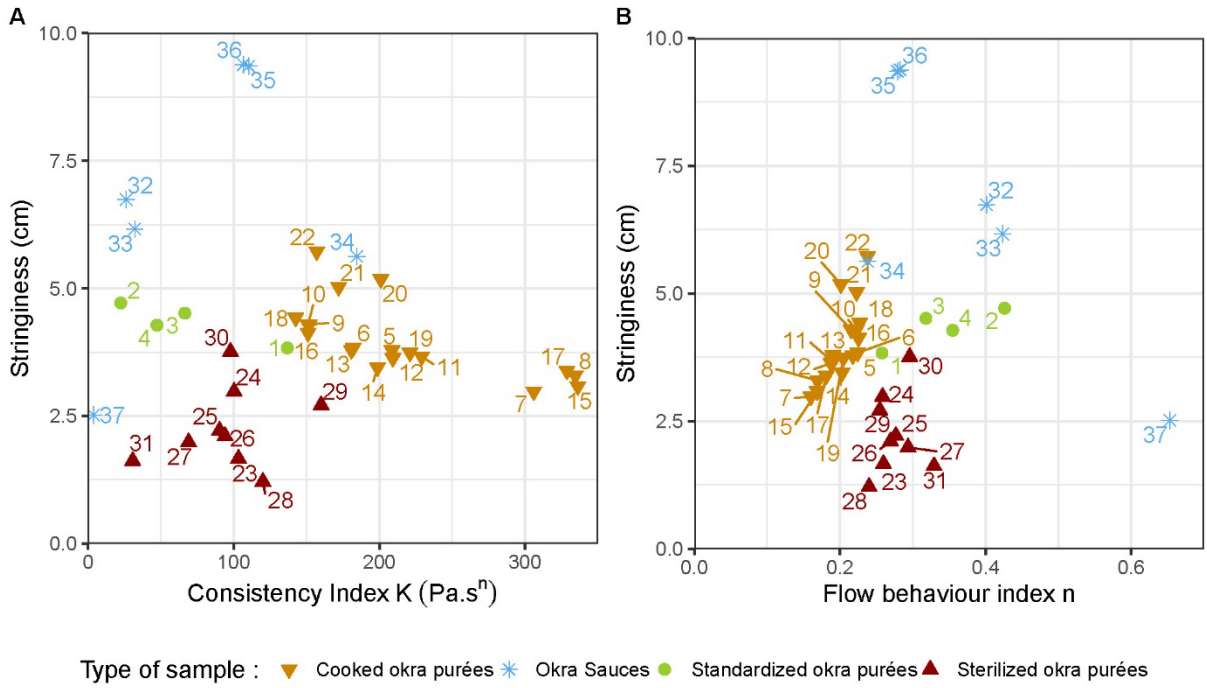

754

755

Figure 11 : Water-dependence of flow consistency index K (A), flow behaviour index n (B) and stringiness (C) for the 37 suspensions